

Combination treatment with perifosine and MEK-162 demonstrates synergism against lung cancer cells *in vitro* and *in vivo*

Jianli Zhang · Yue Hong · Jie Shen

Received: 16 January 2015 / Accepted: 9 February 2015 / Published online: 20 February 2015
© International Society of Oncology and BioMarkers (ISOBM) 2015

Abstract Lung cancer is a global health problem. The search for new therapeutic approaches for the treatment of lung cancer is important. Here, we reported that the AKT inhibitor perifosine and the MEK/ERK inhibitor MEK-162 synergistically induced lung cancer cell (A549 and H460 lines) growth inhibition and apoptosis. The combined efficiency was significantly higher than either agent alone. For the molecular study, perifosine and MEK-162 worked together to concurrently block AKT, mammalian target of rapamycin (mTOR) complex 1 (mTORC1), and MEK-ERK signalings in lung cancer cells, while either agent alone only affected one or two signalings with lower efficiency. *In vivo*, MEK-162 and perifosine co-administration dramatically inhibited A549 lung cancer xenograft growth, without inducing apparent toxicities. The synergistic activity *in vivo* was again superior than either agent alone. Thus, perifosine and MEK-162 combination is biologically plausible by acting through effects on different proliferation and survival-related signaling pathways. Our *in vitro* and *in vivo* results support the feasibility of investigating the synergism regimen in clinical tests.

Keywords Lung cancer · Perifosine · MEK-162 · PI3K-AKT-mTOR · MEK-ERK · Synergism

Abbreviations

ELISA	Enzyme-linked immunosorbent assay
ERK	Extracellular regulated kinase
FBS	Fetal bovine serum

J. Zhang · Y. Hong
Department of Respiratory Diseases, The First Affiliated Hospital of Zhejiang University, Hangzhou, China

J. Shen (✉)
Department of Pediatrics, the First Affiliated Hospital of Zhejiang University, No. 79 Qingchun Road, Hangzhou 310003, China
e-mail: drshenjierres6@163.com

mTOR	Mammalian target of rapamycin
mTORC1	Mammalian target of rapamycin (mTOR) complex 1
NSCLCs	Non-small cell lung cancers
PI3K	Phosphatidylinositol-3-kinase
PVDF	Polyvinylidene fluoride
RCC	Renal cell carcinoma

Introduction

Lung cancer, especially the non-small cell lung cancers (NSCLCs), is a global health problem [1, 2]. It is one of the leading causes of cancer-caused mortalities in China or around the world [1, 2]. The vast majority of NSCLCs and other lung cancers are detected at advanced stages with local or distant metastasis, making surgical resection almost impossible [1, 3]. Meanwhile, many advanced NSCLCs are resistant to almost all clinically applied chemotherapy drugs [1, 3]. As such, the search for new targets and new therapeutic approaches for the treatment of NSCLCs is urgent [4].

The protein kinase AKT is the central member of the phosphatidylinositol-3-kinase (PI3K)/AKT and the mammalian target of rapamycin (mTOR) pathway, which is frequently dysregulated and constitutively activated in lung cancers and many other cancers, causing cancer progression [4–6]. Further, AKT has other downstream molecular targets independent of mTOR regulating key cancerous processes, ranging from proliferation and survival to metabolism [4–7]. It represents a vital target for NSCLCs and lung cancer prevention [4].

Perifosine, a third-generation alkylphospholipid, was first reported by Kondapaka et al. as a novel AKT inhibitor at pharmacologically relevant concentrations [8]. Perifosine was shown to block AKT translocation to the plasma membrane through interacting its PH domain, and to inhibit AKT

phosphorylation [8–10]. This novel first-in-class oral AKT inhibitor, alone or in combination with other anti-cancer agents, was tested in multiple tumor cell lines both in vivo and in vitro [9–15]. It was also examined in several clinical studies, showing promising results in renal cell carcinoma (RCC) and neuroblastoma [9, 10].

One potential avenue to improve therapeutic index in NSCLCs and other lung cancers might combine agents targeting distinct growth/survival regulatory pathways [1]. This might lead to concurrent inhibition of multiple cancer-promoting signalings, achieving superior anti-lung cancer activity [1]. MEK-162, also known as ARRY-438162, is a potent, selective, and non-ATP-competitive allosteric inhibitor of MEK [16, 17]. It is manufactured by Almac Pharma Services (Craigavon, UK) for Novartis [17]. Preclinical studies have demonstrated that MEK-162, alone or in combination with other anti-cancer agents, has the ability to inhibit growth of melanoma and several other solid tumor cells in vitro and in vivo [18–20]. Phase 1 and phase 2 clinical studies have reported the safety profile of MEK-162 and its anti-tumor activity in patients with NRAS-mutated melanoma [17]. In the current study, we found that combined treatment with perifosine and MEK-162 demonstrates significant synergism against lung cancer cells both in vitro and in vivo.

Materials and methods

Chemicals and reagents

Perifosine and MEK-162 were purchased from Selleck (Shanghai, China). Z-VAD-FMK, Z-DEVD-FMK, and Z-ITED-fmk were purchased from Calbiochem (Shanghai, China).

Antibodies

Antibodies against phospho(p)-AKT (Ser 473), p-S6K1 (Ser 389), p-S6 (Ser 235/236), p-MEK1/2 (Ser 217/221), and p-ERK1/2 (Thr 202/Tyr 204) were purchased from Cell Signaling Tech (Denver, MA). Anti-AKT1, S6K1, S6, ERK1/2, and MEK1/2 were purchased from Santa Cruz (Santa Cruz, CA).

Cell culture

A549 and H460 human lung cancer cell lines were purchased from the Cell Bank of Chinese Academy of Sciences (Shanghai, China). Cells were cultured in DMEM/RPMI medium supplemented with 10 % fetal bovine serum (FBS: HyClone, Shanghai, China) with antibiotics, and incubated at 37 °C in a humidified air atmosphere containing 5 % CO₂. For experiments in which cells were deprived of serum

overnight, cell monolayers were washed with RPMI 1640 containing 2 mM L-glutamine and incubated in the same medium. DNA fingerprinting and profiling were performed every 6 months to confirm the origin of the cell line and to distinguish the cell line from cross-contamination. All cell lines were subjected to mycoplasma and microbial contamination examination every month. Population doubling time, colony forming efficiency, and morphology under phase contrast were also measured every 6 months under defined conditions to confirm the phenotype of the cell line.

Cell growth MTT assay

As previous reported [21, 22], cell growth was measured by the 3-(4,5-dimethylthiazol-2-yl)-2,5-diphenyltetrazolium bromide (MTT) assay. Cells were collected and seeded in 96-well plates at a density of 5×10^3 cells/well. After treatment, MTT tetrazolium salt (0.5 mg/ml, Sigma, St. Louis, MO) was added to culture well for 4 h. Then, DMSO (150 μ l/well) was added to dissolve formazan crystals: the absorbance of each well was observed by a plate reader at a test wavelength of 490 nm with a reference wavelength of 630 nm.

Colony formation assay

For clonogenic assays, A549 cells or H460 cells were plated at a density of 3000 cells/well in 2 ml of medium. After overnight attachment, cells were treated with indicated agents. Colony formation was determined after 7 days, and the number of colonies was manually counted.

Measurement of apoptosis

A549 cells or H460 cells were plated at a density of 400,000 cells/well in six-well plates. After treatment, both the floating cells and attached cells were pooled after trypsinization, fixed in 70 % ethanol, and stored at -20° prior to analysis. Apoptotic cells were detected as Annexin-FITC (Becton Dickinson, Shanghai, China) positive cells using a Becton Dickinson FACScan (Shanghai, China).

Histone-DNA enzyme-linked immunosorbent assay (ELISA) assay

Cell apoptosis was quantified by histone-DNA ELISA (Roche Applied Science, Shanghai, China) according to manufacturer's protocol. Briefly, the cytoplasmic histone-DNA fragments from cells were extracted and bound to the immobilized anti-histone antibody. Subsequently, the peroxidase-conjugated anti-DNA antibody was added for the detection of immobilized histone-DNA fragments. After addition of substrate for peroxidase, the spectrophotometric absorbance

of the samples was determined using a plate reader at a test wavelength of 400 nm.

Western blots

As reported [21, 22], cells with indicated treatment were harvested in the lysis buffer (Jingmei Biotech, Shanghai, China). The protein concentration was determined by Bio-Rad protein assay (Bio-Rad, Beijing, China). Aliquots of 30 µg of lysates per sample were electrophoresed on 10 % SDS-PAGE gel and transferred to a polyvinylidene fluoride (PVDF) membrane. The blot was incubated in the blocking buffer and then incubated with the primary antibody at 4 °C overnight with PBST. Appropriate secondary antibody conjugated to horseradish peroxidase (HRP) was then added. Antigen-antibody complex was detected by using enhanced chemiluminescence (ECL) reagent. The blot intensity was quantified through the ImageJ software.

A549 tumor xenograft model in nude mice

Female nude mice were applied to establish xenograft tumor model of A549 cells. A549 cells (3.5 million cells in 0.2 ml of culture medium) were subcutaneously injected at the left thigh of nude mice, and treatment was started when the tumors reached an average volume of 200~300 mm³. Mice were ear tagged and randomized into four groups: vehicle, perifosine (1 mg/kg, lavage, once daily), MEK-162 (2.5 mg/kg, lavage, once daily), and perifosine+MEK-162, with five mice per group. The mice were examine daily for toxicity/mortality relevant to treatment, and the tumor volume was measured with a caliper once every week for up to 4 weeks. The tumor volume (in mm³) was calculated by the formula as follows: volume=(width)²×length/2, and the tumor growth curve was presented. At the end of the experiment, tumor xenograft was isolated, tumor weight was measured. All studies were performed in accordance with the standards of ethical treatment approved by the Institutional Animal Care and Use Committee (IACUC) and Association for the Assessment and Accreditation of Laboratory Animal Care (AAALAC). The protocols of the in vivo study were approved by the Animal Care and Use Committee at all authors institutions.

Data analysis

The data were expressed as means±Stand error (SE). Data were collected using a minimum of three experiments. Statistical differences were analyzed by one-way ANOVA followed by multiple comparisons performed with post hoc Bonferroni test (SPSS version 15). Values of $p < 0.05$ were considered statistically significant.

Results

In vitro perifosine and MEK-162 synergism in lung cancer cells

We first examined potential synergism between perifosine and MEK-162 in cultured lung cancer cells (A549 and H460 lines). As shown in Fig. 1a–b, the growth inhibitory effect of perifosine at tested concentration (0.3–10 µM) was relatively weak in A549 cells. However, in the presence of MEK-162, its anti-growth activity was significantly increased for the same intervals (24 h/72 h) (Fig. 1a–b). For example, the 50 % growth inhibition (GI-50) for perifosine (72 h) decreased from 13.52 to 0.731 µM with the co-treatment of MEK-162 in A549 cells (Fig. 1a–b). Note that MEK-162 alone only slightly affected the growth of A549 cells, only resulting in less than 20 % MTT OD reduction at 72 h (Fig. 1a–b). Further, perifosine (3 µM) and MEK-162 (1 µM) synergistically inhibited A549 cell colony formation, the synergistic activity was superior than either agent alone (Fig. 1c). In vitro perifosine and MEK-162 synergism was also observed in H460 lung cancer cells. In the presence of MEK-162 (1 µM), the activity of perifosine on H460 cell growth (Fig. 1d–e) and colony formation (Fig. 1f) was significantly enhanced. Together, these results demonstrated the in vitro synergism between perifosine and MEK-162 in lung cancer cells.

Perifosine and MEK-162 synergistically induce lung cancer cell apoptosis

Decreased cell growth after applied treatment could be a result of increased apoptosis. Thus, we tested the effect of perifosine and/or MEK-162 on lung cancer cell apoptosis. Results from the Annexin V FACS assay showed that perifosine at the concentration of 1–3 µM only slightly induced A549 cell apoptosis, with less than 10–15 % apoptotic cells (Fig. 2a). Co-administration with MEK-162 increased cell apoptosis induction by perifosine, resulting in over 20–25 % of A549 cell apoptosis (Fig. 2a). MEK-162 alone only slightly affected A549 cell apoptosis (Fig. 2a). Histone-DNA ELISA apoptosis assay further confirmed the synergistic effect between perifosine and MEK-162 in promoting A549 cell apoptosis (Fig. 2b). Similar synergism of the two agents in activating cell apoptosis was also observed in H460 cells (Fig. 2c–d). To study the role of apoptosis in co-administration-mediated growth inhibition, three different apoptosis inhibitors, including Z-VAD-FMK (a general caspase inhibitor), Z-DEVD-FMK (inhibitor of caspases 3,6,7,8,10), and Z-ITED-fmk (specific inhibitor of caspase 8), were applied. Results showed all these inhibitors significantly reduced co-treatment-induced growth inhibition in both A549 cells (Fig. 2e) and H460 cells (Fig. 2f). Thus, synergistic growth inhibition by the co-

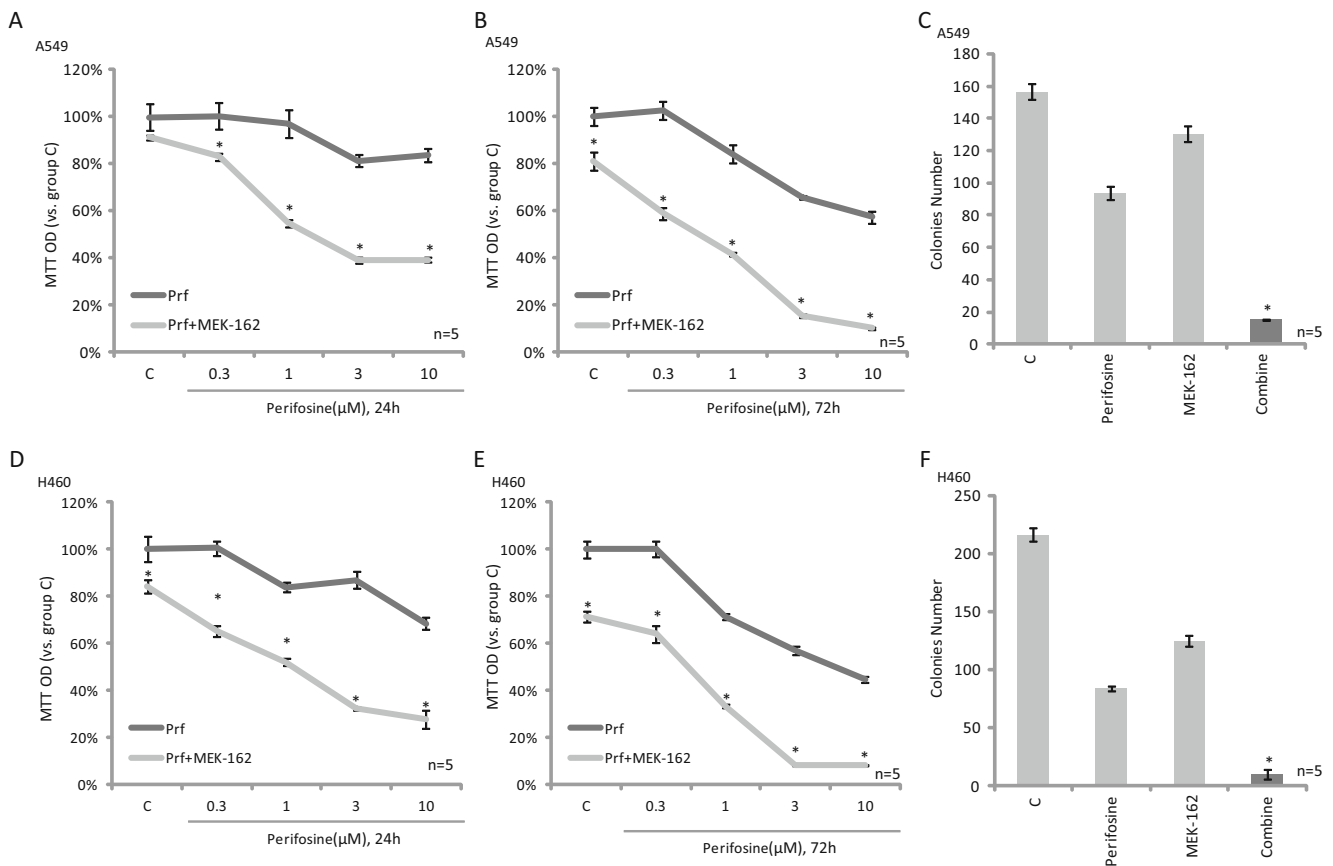


Fig. 1 Effect of perifosine and MEK-162 on lung cancer cell growth. Human lung cancer A549 cells or H460 cells were untreated (C), or treated with indicated concentration of perifosine (0.3–10 μ M), in the presence or absence of MEK-162 (1 μ M); for 24 (a, d) or 72 h (b, e), cell growth was tested by MTT assay. A549 cells (c) and H460 cells (f) were either left untreated (C), treated with perifosine (3 μ M), MEK-162

(1 μ M), or combination; colony formation assay was performed as described. *Prf* stands for perifosine. The results presented are representative of three independent experiments. The values were expressed as the means \pm SE. * p <0.05 compared with group without MEK-162 co-treatment

treatment could be due to apoptosis activation in lung cancer cells.

Perifosine and MEK-162 concurrently blocks AKT, mTORC1, and ERK-MAPK activation

We also tested the signaling changes in lung cancer cells treated with perifosine and/or MEK-162. Perifosine is a well-established AKT inhibitor [9, 10]. Here, perifosine (3 μ M) also blocked AKT activation in A549 cells (Fig. 3a). Perifosine showed no significant effect on MEK-ERK1/2 phosphorylation in A549 cells (Fig. 3b), and a relatively weak effect on mTORC1 activation; the latter was indicated by phospho-S6K1 and S6 (Fig. 3c). Significantly, perifosine and MEK-162 co-administration not only blocked AKT (Fig. 3a) and MEK-ERK phosphorylation (Fig. 3b) but also abolished mTORC1 activation (S6K1 and S6 phosphorylations) (Fig. 3c). MEK-162 alone only slightly inhibited S6K1-S6 phosphorylation and blocked ERK1/2 phosphorylation (Fig. 3c). Similar signaling results were also observed in H460 cells, while perifosine and MEK-162 co-treatment

blocked AKT (Fig. 3d), MEK-ERK (Fig. 3e), and mTORC1 (Fig. 3f) activation. Although there are studies showing that perifosine induces autophagic degradation of regular (total) AKT and major components of mTOR axis [23], that effect by perifosine is dose and cell line dependent [23]. Here, we found that regular AKT, S6K, and S6 were not affected by applied perifosine treatment in tested cell lines (Fig. 3). Regular ERK and MEK were also not affected by perifosine (Fig. 3), which is consistent with other studies [22, 24]. Further, these regular kinases were also not downregulated by MEK-162 (Fig. 3). Together, these results showed that perifosine and MEK-162 worked together to concurrently block AKT, mTORC1, and ERK-MAPK activation in lung cancer cells.

In vivo perifosine and MEK-162 synergism against A549 xenograft

At last, we tested the possible perifosine and MEK-162 synergism in vivo. A549 lung cancer xenograft model was applied. In consistent with the in vitro results, tumor growth

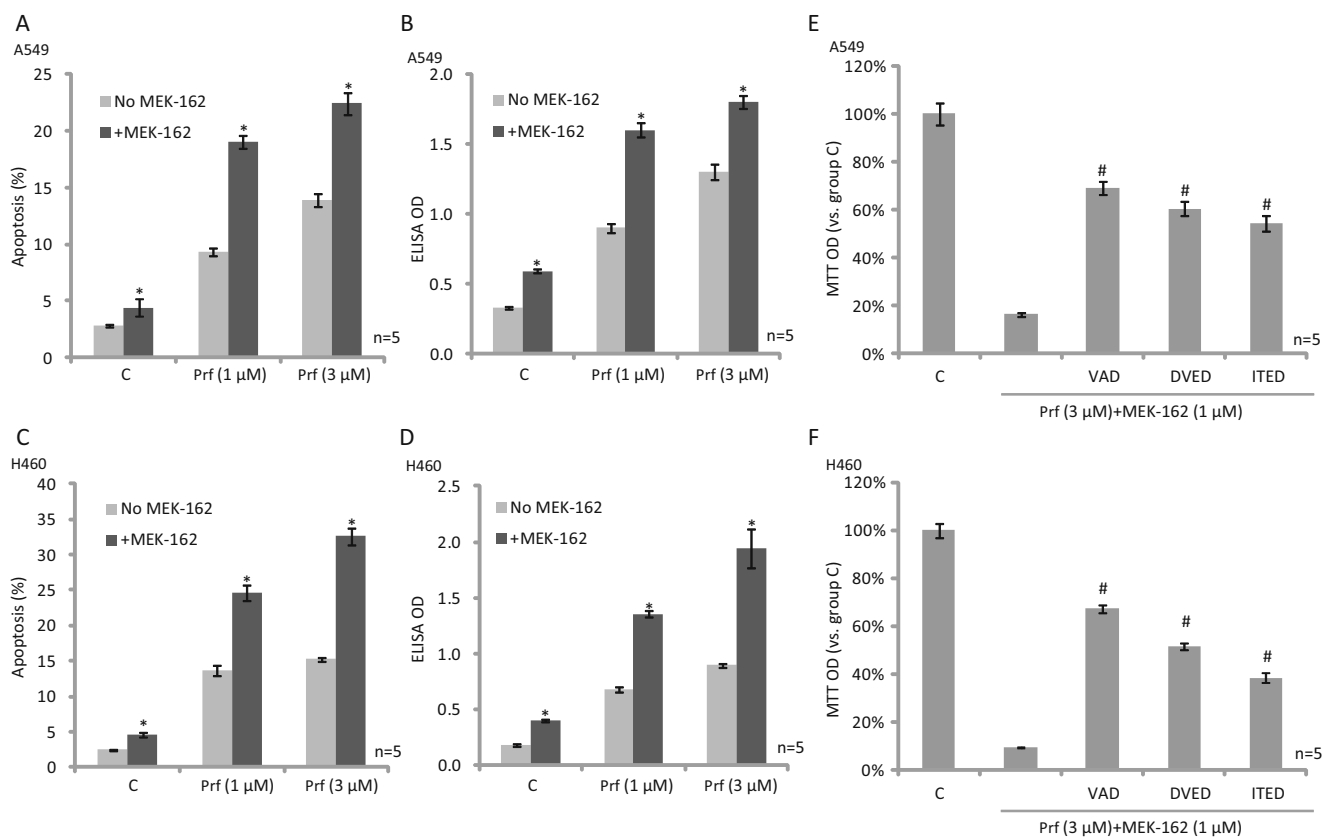


Fig. 2 Effect of perifosine and MEK-162 on lung cancer apoptosis. A549 cells (a–b) and H460 cells (c–d) were treated with indicated concentration of perifosine (1–3 μ M), in the presence or absence of MEK-162 (1 μ M); for 48 h, cell apoptosis was tested by either Annexin V FACS assay or histone-DNA apoptosis ELISA assay. A549 cells (e) and H460 cells (f) were pretreated with VAD-fmk (VAD, 40 μ M), Z-DEVD-FMK (DVED, 40 μ M), or Z-ITED (ITED, 40 μ M) for 1 h,

followed by perifosine (3 μ M) plus MEK-162 (1 μ M) co-stimulation; cell growth was tested by MTT assay after 72 h. C stands for untreated control group. The results presented are representative of three independent experiments. The values were expressed as the means \pm SE. * p <0.05 compared with group without MEK-162 (a–d). # p <0.05 compared with the co-treatment group

curve results in Fig. 4a showed that only mice group administrated with both perifosine and MEK-162 demonstrated with dramatically inhibited A549 xenograft growth. Tumor mass weight results further confirmed the perifosine and MEK-162 synergism in vivo (Fig. 4b). Perifosine or MEK-162 alone exerted a relatively weak but significant inhibitory effect on A549 xenograft growth at weeks 3–4 (Fig. 4a). Further, as a single agent, perifosine or MEK-162 also decreased tumor weight, although the effect of MEK-162 was not significant (P >0.05 vs. vehicle group) (Fig. 4b). Significantly, in the experimental mice administrated with indicated perifosine and/or MEK-162, no significant adverse effects, including dermatitis, peripheral edema, facial edema, diarrhea, or vomiting, were observed. Meanwhile, the mice body weight was not affected by perifosine and/or MEK-162 administration (Fig. 4c). Thus, this regimen is relatively safe at least in nude mice. Together, we show that perifosine and MEK-162 synergistically inhibit A549 xenograft growth in vivo.

Discussions

Perifosine is a first-in-class oral alkylphospholipid AKT inhibitor exhibiting anti-tumor properties, and it is currently under phase II–III clinical trials for various types of cancer [9, 10]. The mechanisms by which perifosine exerts its anti-tumor effects, including the induction of apoptosis, are not fully understood [9, 10]. Here, we found that perifosine alone exerted a relatively weak activity against lung cancer cells in vitro and in vivo, partly because it had no or weak effect on other important pro-growth/survival pathways: MEK/ERK and mTORC1 signalings. Significantly, co-administration with MEK-ERK inhibitor MEK-162 dramatically sensitized perifosine's activity and led to substantial lung cancer cell apoptosis.

The complexity of the cellular signaling network in cancer cells opens the opportunity to combine perifosine with other pro-cancer pathways that are not directly affected by

Fig. 3 Effect of perifosine and MEK-162 on AKT, mTORC1, and MEK-ERK signalings. A549 cells (a–c) or H460 cells (d–f) were either left untreated (C), treated with perifosine (3 μ M), MEK-162 (1 μ M), or combine for 8 h; expression of indicated proteins was tested by Western blots using corresponding antibodies. Protein phosphorylation was quantified. Experiments were repeated three times, and similar results were obtained

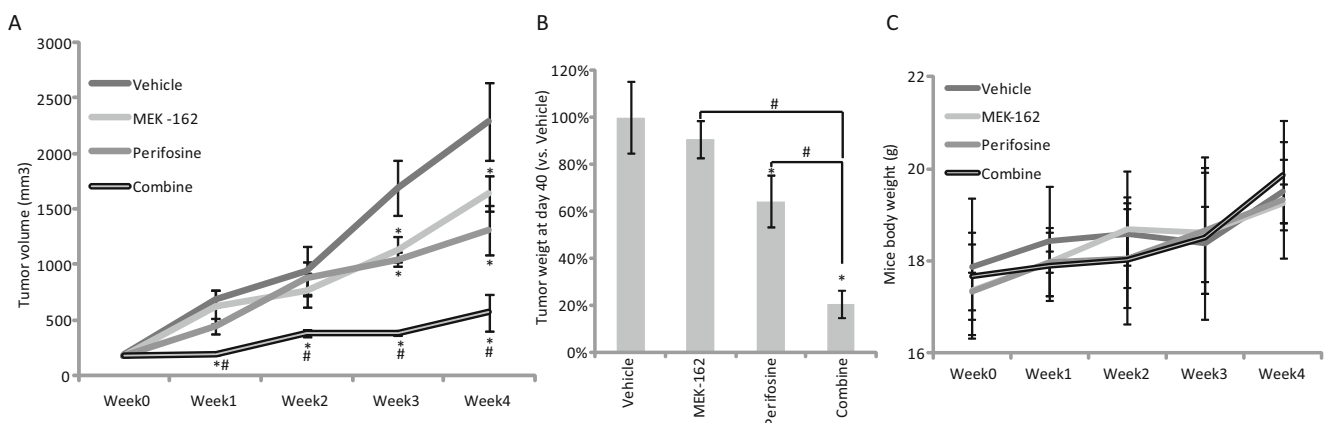
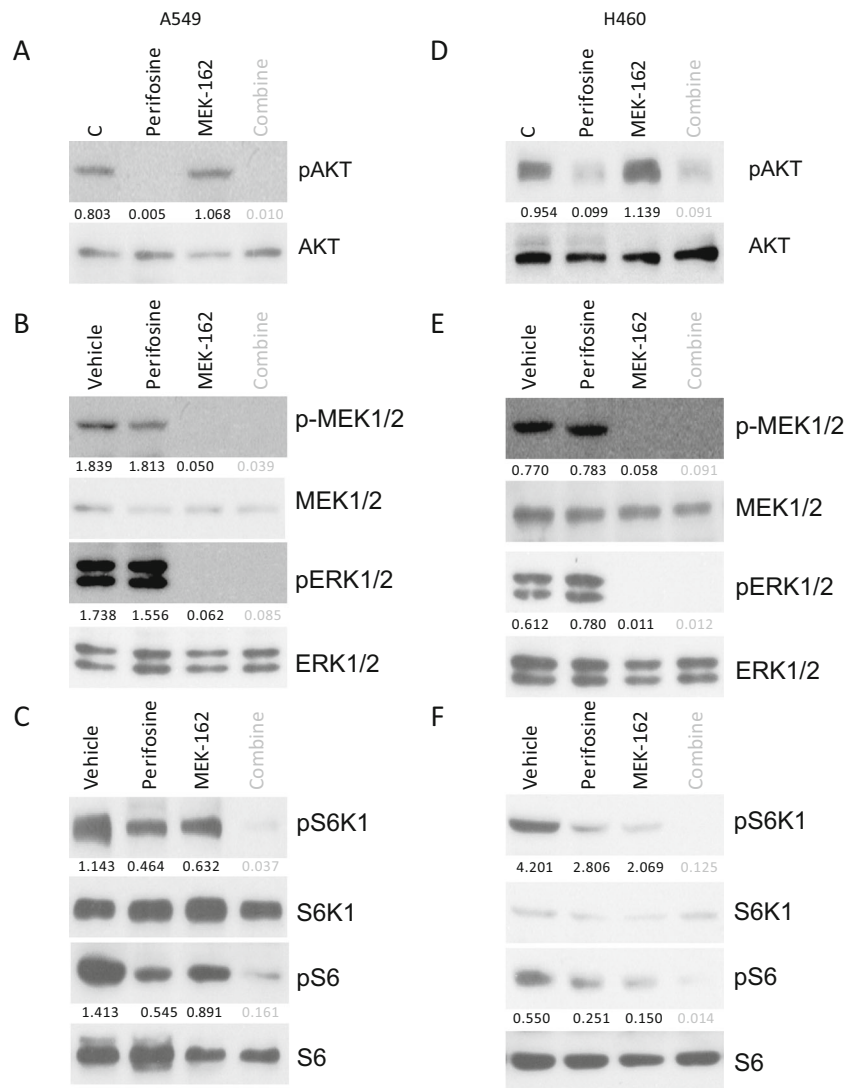


Fig. 4 Effect of perifosine and/or MEK-162 administration on A549 xenograft growth in nude mice. Female nude mice, 18–20 g, 4–6 weeks old, were inoculated s.c. with 3.5×10^6 A549 cells in a volume 0.2 ml culture medium containing 10 % FBS. Drug treatment was initiated 15 days after tumor cell inoculation, when established tumors were around 200 mm³ in volume. Mice were ear tagged and randomized into four groups: vehicle (saline), perifosine (1 mg/kg, lavage, once daily),

MEK-162 (2.5 mg/kg, lavage, once daily), and perifosine+MEK-162, for a total of 14 days with five mice per group. Tumor volume (in mm³, recorded every week) (a), tumor mass weight (vs. vehicle, at the end of experiment) (b), and mice body weight (in grams, recorded every week) (c) were shown. Data were expressed as mean \pm SE, and experiments were repeated three times. * $p < 0.05$ vs. Vehicle group (a, b). # $p < 0.05$ vs. group of MEK-162/perifosine alone (a), # $p < 0.05$ (b)

perifosine [9, 10]. Synergistic effects could be achieved with the combination of these inhibitors [9, 10]. For example, co-administration with perifosine with mTOR inhibitors showed a synergistic activity in multiple myeloma (MM) and glioblastoma [13, 15]. Further, phosphoinositide-dependent kinase-1 (PDK1) inhibitor UCN-01 was synergistic to perifosine in prostate and lung cancer cells [25]. Perifosine acted synergistically with cetuximab or erlotinib, both inhibiting EGF receptor (EGFR), in breast and prostate cancer cells [26, 27]. The obvious advantage using MEK-162 and perifosine synergism in this study is concurrent inhibiting of AKT-mTOR and MEK-ERK signalings.

Recent studies have identified the important role of mTOR in lung cancer initiation and progression [4]. mTOR exists in at least two functionally distinct multi-protein complexes including mTORC1 and mTORC2 [28, 29]. Rapamycin-sensitive mTORC1 is composed of mTOR, Raptor, mLST8, PRAS40, and others, which is responsible for phosphorylation S6K1 and 4E-BP1 [30, 31]. Although AKT is a major upstream kinase for mTORC1, studies have found that other signaling mechanisms could bypass AKT and activate mTORC1 directly [31]. For example, ERK could phosphorylate TSC2 to activate mTORC1 [32, 33]. In the current study, our evidence suggests that both AKT and ERK signalings are possible upstream kinase for mTORC1 activation in tested lung cancer cells. Concurrent inhibition of AKT and ERK by the co-treatment almost blocked mTORC1 activation (S6K1 and S6 phosphorylation), while either agent alone showed a much weaker effect on phosphorylation of S6K1 and S6 in lung cancer cells.

Besides inactivating AKT, perifosine is shown to regulate several additional primary or secondary cellular targets that may affect cell apoptosis/proliferation [9, 10]. For example, perifosine could activate pro-apoptotic JNK in various cancer cell lines [24, 34, 35]. Inhibition of JNK, both pharmacologically or genetically, then alleviated perifosine-induced cancer cell apoptosis [34, 35]. Several studies demonstrated that perifosine could inhibit ERK activation, but that effect was cell line dependent [36, 37]. Reactive oxygen species (ROS) production was also increased in several perifosine-stimulated cancer cell lines [12, 24, 34]. Further, perifosine-induced cell apoptosis was associated with ceramide production [24, 34]. Thus, it is possible that other mechanisms besides AKT-mTOR and MEK-ERK inactivation might also contribute to perifosine and/or MEK-162-induced inhibition on the lung cancer cells.

The results of phase II perifosine combination trials in multiple myeloma (MM) and colorectal cancer were among the most promising activities [10]. However, following phase III clinical studies failed to demonstrate significant clinical advance with the low-dose perifosine scheme in patients with metastatic colorectal cancer and relapsed MM, in combination with capecitabine and bortezomib, respectively [10]. As

described here, perifosine and MEK-162 combination is biologically plausible by acting through effects on different proliferation and survival-related signaling pathways; thus, the *in vitro* and *in vivo* results of this study support the feasibility of investigating the synergistic regimen in clinical tests.

Acknowledgments This work is supported by the National Science Foundation of China.

Conflicts of interest None

References

- Raez LE, Lilenbaum R. Chemotherapy for advanced non-small-cell lung cancer. *Clin Adv Hematol Oncol*. 2004;2:173–8.
- Siegel R, Ma J, Zou Z, Jemal A. Cancer statistics, 2014. *CA Cancer J Clin*. 2014;64:9–29.
- Langer C, Lilenbaum R. Role of chemotherapy in patients with poor performance status and advanced non-small cell lung cancer. *Semin Oncol*. 2004;31:8–15.
- Papadimitrakopoulou V. Development of pi3k/akt/mtor pathway inhibitors and their application in personalized therapy for non-small-cell lung cancer. *J Thorac Oncol*. 2012;7:1315–26.
- Vanhaesebroeck B, Stephens L, Hawkins P. Pi3k signalling: the path to discovery and understanding. *Nat Rev Mol Cell Biol*. 2012;13:195–203.
- Liu P, Cheng H, Roberts TM, Zhao JJ. Targeting the phosphoinositide 3-kinase pathway in cancer. *Nat Rev Drug Discov*. 2009;8:627–44.
- Fruman DA, Rommel C. Pi3k and cancer: lessons, challenges and opportunities. *Nat Rev Drug Discov*. 2014;13:140–56.
- Kondapaka SB, Singh SS, Dasmahapatra GP, Sausville EA, Roy KK. Perifosine, a novel alkylphospholipid, inhibits protein kinase b activation. *Mol Cancer Ther*. 2003;2:1093–103.
- Gills JJ, Dennis PA. Perifosine: update on a novel akt inhibitor. *Curr Oncol Rep*. 2009;11:102–10.
- Fensterle J, Aicher B, Seipelt I, Teifel M, Engel J. Current view on the mechanism of action of perifosine in cancer. *Anti Cancer Agents Med Chem*. 2014;14:629–35.
- Qin LS, Yu ZQ, Zhang SM, Sun G, Zhu J, Xu J, et al. The short chain cell-permeable ceramide (c6) restores cell apoptosis and perifosine sensitivity in cultured glioblastoma cells. *Mol Biol Rep*. 2013;40:5645–55.
- Chen MB, Wu XY, Tao GQ, Liu CY, Chen J, Wang LQ, et al. Perifosine sensitizes curcumin-induced anti-colorectal cancer effects by targeting multiple signaling pathways both *in vivo* and *in vitro*. *Int J Cancer*. 2012;131:2487–98.
- Pitter KL, Galban CJ, Galban S, Tehrani OS, Li F, Charles N, et al. Perifosine and CCI 779 co-operate to induce cell death and decrease proliferation in PTEN-intact and PTEN-deficient PDGF-driven murine glioblastoma. *PLoS One*. 2011;6:e14545.
- Fei HR, Chen G, Wang JM, Wang FZ. Perifosine induces cell cycle arrest and apoptosis in human hepatocellular carcinoma cell lines by blockade of akt phosphorylation. *Cytotechnology*. 2010;62:449–60.
- Cirstea D, Hideshima T, Rodig S, Santo L, Pozzi S, Vallet S, et al. Dual inhibition of akt/mammalian target of rapamycin pathway by nanoparticle albumin-bound-rapamycin and perifosine induces anti-tumor activity in multiple myeloma. *Mol Cancer Ther*. 2010;9:963–75.
- Kusters-Vandeveldel HV, Willemsen AE, Groenen PJ, Kusters B, Lammens M, Wesseling P, et al. Experimental treatment of NRAS-

- mutated neurocutaneous melanocytosis with MEK162, a MEK-inhibitor. *Acta Neuropathol Commun.* 2014;2:41.
17. Ascierto PA, Schadendorf D, Berking C, Agarwala SS, van Herpen CM, Queirolo P, et al. MEK162 for patients with advanced melanoma harbouring NRAS or Val600 BRAF mutations: A non-randomised, open-label phase 2 study. *Lancet Oncol.* 2013;14:249–56.
 18. Thumar J, Shahbazian D, Aziz SA, Jilaveanu LB, Kluger HM. MEK targeting in N-RAS mutated metastatic melanoma. *Mol Cancer.* 2014;13:45.
 19. Akinleye A, Furqan M, Mukhi N, Ravella P, Liu D. MEK and the inhibitors: from bench to bedside. *J Hematol Oncol.* 2013;6:27.
 20. Tong Y, Huang H, Pan H. Inhibition of MEK/ERK activation attenuates autophagy and potentiates pemetrexed-induced activity against HepG2 hepatocellular carcinoma cells. *Biochem Biophys Res Commun.* 2015;456:86–91.
 21. Zhang JL, Xu Y, Shen J. Cordycepin inhibits lipopolysaccharide (LPS)-induced tumor necrosis factor (TNF)-alpha production via activating amp-activated protein kinase (AMPK) signaling. *Int J Mol Sci.* 2014;15:12119–34.
 22. Shen J, Liang L, Wang C. Perifosine inhibits lipopolysaccharide (LPS)-induced tumor necrosis factor (TNF)-alpha production via regulation multiple signaling pathways: New implication for Kawasaki disease (KD) treatment. *Biochem Biophys Res Commun.* 2013;437:250–5.
 23. Fu L, Kim YA, Wang X, Wu X, Yue P, Lonial S, et al. Perifosine inhibits mammalian target of rapamycin signaling through facilitating degradation of major components in the mTOR axis and induces autophagy. *Cancer Res.* 2009;69:8967–76.
 24. Ji C, Yang YL, Yang Z, Tu Y, Cheng L, Chen B, et al. Perifosine sensitizes UVB-induced apoptosis in skin cells: new implication of skin cancer prevention? *Cell Signal.* 2012;24:1781–9.
 25. Dasmahapatra GP, Didolkar P, Alley MC, Ghosh S, Sausville EA, Roy KK. In vitro combination treatment with perifosine and UCN-01 demonstrates synergism against prostate (PC-3) and lung (A549) epithelial adenocarcinoma cell lines. *Clin Cancer Res.* 2004;10:5242–52.
 26. Li X, Luwor R, Lu Y, Liang K, Fan Z. Enhancement of antitumor activity of the anti-EGF receptor monoclonal antibody cetuximab/C225 by perifosine in PTEN-deficient cancer cells. *Oncogene.* 2006;25:525–35.
 27. Festuccia C, Gravina GL, Muzi P, Millimaggi D, Dolo V, Vicentini C, et al. Akt down-modulation induces apoptosis of human prostate cancer cells and synergizes with EGFR tyrosine kinase inhibitors. *Prostate.* 2008;68:965–74.
 28. Dienstmann R, Rodon J, Serra V, Tabernero J. Picking the point of inhibition: a comparative review of PI3K/AKT/mTOR pathway inhibitors. *Mol Cancer Ther.* 2014;13:1021–31.
 29. Zaytseva YY, Valentino JD, Gulhati P, Evers BM. mTOR inhibitors in cancer therapy. *Cancer Lett.* 2012;319:1–7.
 30. Guertin DA, Sabatini DM. Defining the role of mTOR in cancer. *Cancer Cell.* 2007;12:9–22.
 31. Sabatini DM. mTOR and cancer: insights into a complex relationship. *Nat Rev Cancer.* 2006;6:729–34.
 32. Ma L, Chen Z, Erdjument-Bromage H, Tempst P, Pandolfi PP. Phosphorylation and functional inactivation of TSC2 by Erk implications for tuberous sclerosis and cancer pathogenesis. *Cell.* 2005;121:179–93.
 33. Ma L, Teruya-Feldstein J, Bonner P, Bernardi R, Franz DN, Witte D, et al. Identification of S664 TSC2 phosphorylation as a marker for extracellular signal-regulated kinase mediated mTOR activation in tuberous sclerosis and human cancer. *Cancer Res.* 2007;67:7106–12.
 34. Sun H, Yu T, Li J. Co-administration of perifosine with paclitaxel synergistically induces apoptosis in ovarian cancer cells: more than just AKT inhibition. *Cancer Lett.* 2011;310:118–28.
 35. Yao C, Wei JJ, Wang ZY, Ding HM, Li D, Yan SC, et al. Perifosine induces cell apoptosis in human osteosarcoma cells: new implication for osteosarcoma therapy? *Cell Biochem Biophys.* 2013;65:217–27.
 36. Rahmani M, Reese E, Dai Y, Bauer C, Payne SG, Dent P, et al. Coadministration of histone deacetylase inhibitors and perifosine synergistically induces apoptosis in human leukemia cells through Akt and ERK1/2 inactivation and the generation of ceramide and reactive oxygen species. *Cancer Res.* 2005;65:2422–32.
 37. Aarts M, Liu Y, Liu L, Besshoh S, Arundine M, Gurd JW, et al. Treatment of ischemic brain damage by perturbing NMDA receptor- PSD-95 protein interactions. *Science.* 2002;298:846–50.